

# Local Dynamics of a New Four-Dimensional Quadratic Autonomous System

Sengen Hu<sup>1,2</sup>, Liangqiang Zhou<sup>1,2\*</sup>

<sup>1</sup>School of Mathematics, Nanjing University of Aeronautics and Astronautics, Nanjing, China

<sup>2</sup>Key Laboratory of Mathematical Modelling and High Performance Computing of Air Vehicles (NUAA), Nanjing, China

Email: \*zlqrex@sina.com

**How to cite this paper:** Hu, S.G. and Zhou, L.Q. (2022) Local Dynamics of a New Four-Dimensional Quadratic Autonomous System. *Journal of Applied Mathematics and Physics*, 10, 2632-2648.

<https://doi.org/10.4236/jamp.2022.109177>

**Received:** August 2, 2022

**Accepted:** September 11, 2022

**Published:** September 14, 2022

Copyright © 2022 by author(s) and Scientific Research Publishing Inc.

This work is licensed under the Creative Commons Attribution International License (CC BY 4.0).

<http://creativecommons.org/licenses/by/4.0/>



Open Access

## Abstract

In this manuscript, Local dynamic behaviors including stability and Hopf bifurcation of a new four-dimensional quadratic autonomous system are studied both analytically and numerically. Determining conditions of equilibrium points on different parameters are derived. Next, the stability conditions are investigated by using Routh-Hurwitz criterion and bifurcation conditions are investigated by using Hopf bifurcation theory, respectively. It is found that Hopf bifurcation on the initial point is supercritical in this four-dimensional autonomous system. The theoretical results are verified by numerical simulation. Besides, the new four-dimensional autonomous system under the parametric conditions of hyperchaos is studied in detail. It is also found that the system can enter hyperchaos, first through Hopf bifurcation and then through periodic bifurcation.

## Keywords

Four-Dimensional Autonomous System, Routh-Hurwitz Criterion, Hopf Bifurcation, Hyperchaos

## 1. Introduction

Due to some characteristics of chaos, such as the sensitive dependence on initial values and the unpredictability of long-term development, chaos is a special means suitable for information encryption processing. Chaos has great potential in the field of image encryption. So far, the research of chaotic image encryption technology still attracts much attention. Hagra and Saber [1] proposed an implementation of the gray image encryption based on the 4D memristor chaotic system, and demonstrated that the investigated encryption approach can protect high speed and high security against various attack. Zhu *et al.* [2] proposed an

image encryption algorithm combining pixel segmentation operation, block chaotic matrix confusion operation and pixel diffusion operation with sinusoidal polynomial composite chaotic system, which has the advantages and effectiveness of image encryption algorithm. Based on a sliding-mode-based controller designed for finite-time synchronization of memristor chaotic systems, Li *et al.* [3] proposed and implemented a new image encryption algorithm. Xian *et al.* [4] studied an encryption method with spatiotemporal chaotic system based on double parameters fractal sorting vector. Guo *et al.* [5] studied image encryption of the chaotic systems generated by quadratic functions topologically conjugate with Logistic map and Tent map, which is poor in resisting the chosen plaintext attack. Hyperchaos has better performance in image encryption than chaos. Image encryption technology based on hyperchaos and other current technologies has been more widely studied by scholars. An improved image encryption algorithm based on hyperchaotic systems and random walk is proposed by Fan *et al.* [6], which does not have only the original advantages, but can also improve the ability to resist attacks. Li *et al.* [7] proposed an image encryption scheme combining neural network, domain diffusion and fractional-order laser hyperchaos system, which offers a new research perspective for optical image encryption. Samiullah *et al.* [8] demonstrated that mostly encryption algorithm based on DNA computing and multiple Chaotic Systems has enhanced performance as compared to contemporary works in information security. Liu *et al.* [9] proposed an image encryption scheme that combines 5D hyperchaos system with DNA technology, and verified that the scheme can achieve good encryption effect and resist various attacks. Gao *et al.* [10] designed a multi-image encryption scheme based on the fractional-order hyperchaotic system and multiple image fusion, which increases the efficiency of image encryption and transmission.

Hopf bifurcation is one of many bifurcation types, which plays an important role in the analysis of complex systems. Lv [11] analyzed a diffusion system with memory delay and general delay by studying its Hopf bifurcation. Efran and Manuel [12] addressed the problem of a robust tracking, surveillance and landing of a mobile ground target by Hopf bifurcation. Li *et al.* [13] studied an improved wheelset motion model with two degrees of freedom through Hopf bifurcation method. By analyzing the existence of Hopf bifurcation, Wang *et al.* [14] studied a delayed diffusive predator-prey model with predator interference or foraging facilitation. Huang *et al.* [15] investigated a diffusive complex Ginzburg-Landau model with delayed feedback and phase shift by discussing conditions for the existence of resonant double Hopf bifurcation. Hopf bifurcation is also a way to enter chaos, so it is often used to study some chaotic systems. Dealing with chaotic fractional-order system in the sense of the Caputo fractional derivative with entanglement function, Shiva *et al.* [16] derived conditions under which the system undergoes a Hopf bifurcation. Wang *et al.* [17] discussed a tumor and Lymphatic immune system interaction model with two time delays, in which Hopf bifurcation describes the chaotic attractor formation. Ramesh *et al.* [18] studied Hopf bifurcation of a fractional-order butterfly-fish chao-

tic system and derived the existence of a chaotic attractor in the system. Amin and Saeed [19] presented a four-dimensional quadratic autonomous hyper-chaotic system and analyzed the local dynamics of stability and Hopf bifurcation. Hopf bifurcation of a Lorenz type system [20] and the Repressilator Model [21] were investigated by Calderon-Saavedra *et al.* and Verdugo, respectively.

The rest of the manuscript consists of five sections. The new four-dimensional quadratic autonomous system and its equilibriums are derived in Section 2. Stability condition of each equilibrium point is derived in Section 3. Hopf bifurcation is studied in Section 4. Numerical simulations are shown in Section 5. The conclusions are drawn in Section 6.

## 2. Dynamic Modeling

Recently, Fang *et al.* [22] proposed a hyperchaotic system and studied its image encryption. Based on this system, a new four-dimensional quadratic autonomous system is presented as follows

$$\begin{cases} \dot{x} = ay - ax + z, \\ \dot{y} = bx - y - xz, \\ \dot{z} = x^2 - cz, \\ \dot{w} = -w + dy^2. \end{cases} \quad (1)$$

where  $(x, y, z, w) \in \mathbb{R}^4$ ,  $a, b, c, d \in \mathbb{R}$ , are constant parameters, determining dynamic behaviors of the system (1).

When  $a + c > -2$ , the system (1) is dissipativity and symmetrical about  $z$ - $w$  plane, for  $\nabla V = \frac{\partial \dot{x}}{\partial x} + \frac{\partial \dot{y}}{\partial y} + \frac{\partial \dot{z}}{\partial z} + \frac{\partial \dot{w}}{\partial w} = -(a + c + 2) < 0$  and invariance under local coordinate transformation:  $(-x, -y, z, w) \rightarrow (x, y, z, w)$ .

The equilibrium points of system (1) can be described in the following theorem:

**Theorem 1.** *The equilibrium points of the system (1) depends on parameters  $a, b, c$ , which are illustrated as follows.*

1) If the system parameters satisfy the following condition

$$\frac{a}{c} \neq 0, \quad 1 + 4a^2(b-1)c < 0, \quad (2)$$

then there is only one equilibrium point  $X_0 = (0, 0, 0, 0)$ .

2) If the system parameters satisfy the following condition

$$\frac{a}{c} \neq 0, \quad 1 + 4a^2(b-1)c = 0, \quad (3)$$

then there are two equilibrium points  $X_0 = (0, 0, 0, 0)$  and  $X_1 = (x_1, y_1, z_1, w_1)$ ,

where  $x_1 = \frac{1}{2a}$ ,  $y_1 = \frac{2a^2c-1}{4a^3c}$ ,  $z_1 = 1-b$ ,  $w_1 = (1-b)(2b-1)^2cd$ .

3) If the system parameters satisfy the following condition

$$\frac{a}{c} \neq 0, \quad 1 + 4a^2(b-1)c > 0, \quad (4)$$

then there are three equilibrium points  $X_0 = (0, 0, 0, 0)$ ,  $X_2 = (x_2, y_2, z_2, w_2)$ , and

$$X_3 = (x_3, y_3, z_3, w_3), \text{ where } x_2 = \frac{1 - \sqrt{\Delta}}{2a}, y_2 = \frac{2a^2c(1 - \sqrt{\Delta}) - (1 - \sqrt{\Delta})^2}{4a^3c},$$

$$z_2 = \frac{(1 - \sqrt{\Delta})^2}{4a^2c}, w_2 = \frac{d(2a^2bc - 2a^2c + 1 - \sqrt{\Delta})(2a^2c - 1 + \sqrt{\Delta})}{4a^4c}, \text{ and}$$

$$x_3 = \frac{1 + \sqrt{\Delta}}{2a}, y_3 = \frac{2a^2c(1 + \sqrt{\Delta}) - (1 + \sqrt{\Delta})^2}{4a^3c}, z_3 = \frac{(1 + \sqrt{\Delta})^2}{4a^2c},$$

$$w_3 = \frac{d(2a^2bc - 2a^2c + 1 + \sqrt{\Delta})(2a^2c - 1 - \sqrt{\Delta})}{4a^4c}, \text{ and } \Delta = \frac{1 + 4a^2(b-1)c}{c^2}.$$

**Proof 1.** Letting the right terms of Equation (1) equal zero, one can obtain that

$$\begin{cases} y = bx - \frac{1}{c}x^3, \\ z = \frac{1}{c}x^2, \\ w = b^2dx^2 - \frac{2bd}{c}x^4 + \frac{d}{c^2}x^6. \end{cases} \quad (5)$$

and

$$a(b-1)x + \frac{1}{c}x^2 - \frac{a}{c}x^3 = 0. \quad (6)$$

If condition (1) is satisfied, then  $\frac{a}{c} \neq 0$  and  $\Delta < 0$ . So Equation (6) has only one root  $x_0 = 0$ . Substituting to Equation (5), one can get there is only one equilibrium point  $X_0$ ;

If condition (2) is satisfied, then  $\frac{a}{c} \neq 0$  and  $\Delta = 0$ . So Equation (6) has two roots  $x_0 = 0$ ,  $x_1 = \frac{1}{2a}$ . Substituting to Equation (5), one can get there are two equilibrium points  $X_0$  and  $X_1$ ;

If condition (3) is satisfied, then  $\frac{a}{c} \neq 0$  and  $\Delta > 0$ . So Equation (6) has three roots  $x_0 = 0$ ,  $x_2 = \frac{1 - \sqrt{\Delta}}{2a}$ ,  $x_3 = \frac{1 + \sqrt{\Delta}}{2a}$ . Substituting to Equation (5), one can get there are three equilibrium points  $X_0$ ,  $X_2$  and  $X_3$ .

Therefore, theorem 1 is deduced.

### 3. Stability Analysis

In this section, the stability of the equilibrium points of system (1) is respectively studied.

#### 3.1. Equilibrium Point $X_0$

First of all, the initial equilibrium  $X_0$  is considered. The Jacobian matrix of

system (1) at  $X_0$  is evaluated as

$$A_0 = \begin{bmatrix} -a & a & 1 & 0 \\ b & -1 & 0 & 0 \\ 0 & 0 & -c & 0 \\ 0 & 0 & 0 & -1 \end{bmatrix}. \quad (7)$$

By calculation, it is obtained that the characteristic equation of the Jacobian matrix  $A_0$  as follows

$$\lambda^4 + R_1\lambda^3 + R_2\lambda^2 + R_3\lambda + R_4 = 0, \quad (8)$$

where

$$\begin{aligned} R_1 &= a + c + 2, & R_2 &= -ab + ac + 2a + 2c + 1, \\ R_3 &= -abc - ab + 2ac + a + c, & R_4 &= -abc + ac. \end{aligned} \quad (9)$$

The eigenvalues of the Jacobian matrix  $A_0$  are characterized as follows:

$$\lambda_1 = -1, \quad \lambda_2 = -c, \quad \lambda_{3,4} = -\frac{1+a}{2} \pm \frac{1}{2}\sqrt{a^2 + 4ab - 2a + 1}. \quad (10)$$

If the following conditions are satisfied:

$$c > 0, \quad a^2 + 4ab - 2a + 1 < 0, \quad (11)$$

or

$$c > 0, \quad -\frac{1+a}{2} \pm \frac{1}{2}\sqrt{a^2 + 4ab - 2a + 1} < 0, \quad (12)$$

then all the eigenvalues of matrix  $A_0$  have negative real parts, so the equilibrium point  $X_0$  is asymptotically stable.

### 3.2. Equilibrium Point $X_1$

In the subsection, the equilibrium point  $X_1$  is considered. The Jacobian matrix of system (1) at  $X_1$  is evaluated as

$$A_1 = \begin{bmatrix} -a & a & 1 & 0 \\ 2b-1 & -1 & -\frac{1}{2a} & 0 \\ \frac{1}{a} & 0 & -c & 0 \\ 0 & \frac{(2a^2c-1)d}{2a^3c} & 0 & -1 \end{bmatrix} \quad (13)$$

By calculation, it is obtained that the characteristic equation of the Jacobian matrix  $A_1$  is as follows

$$\hat{\lambda}^4 + \hat{R}_1\hat{\lambda}^3 + \hat{R}_2\hat{\lambda}^2 + \hat{R}_3\hat{\lambda} + \hat{R}_4 = 0, \quad (14)$$

where

$$\begin{aligned} \hat{R}_1 &= a + c + 2, & \hat{R}_2 &= -2ab + ac + 3a + 2c + 1 - \frac{1}{a}, \\ \hat{R}_3 &= -2abc - 2ab + 3ac + 2a + c - \frac{3}{2a}, & \hat{R}_4 &= -2abc + 2ac - \frac{1}{2a}. \end{aligned} \quad (15)$$

Due to complexity and length of the eigenvalues of the Jacobian matrix  $A_1$ , the Routh-Hurwitz criterion is adopted.

According to the Routh-Hurwitz criterion, if the following conditions are satisfied:

$$\hat{R}_1 > 0, \quad \hat{R}_1 \hat{R}_2 - \hat{R}_3 > 0, \quad \hat{R}_1 \hat{R}_2 \hat{R}_3 - \hat{R}_3^2 - \hat{R}_1^2 \hat{R}_4 > 0, \quad \hat{R}_4 > 0 \quad (16)$$

then all the eigenvalues of matrix  $A_1$  have negative real parts, so the equilibrium point  $X_1$  is asymptotically stable.

### 3.3. Equilibrium Point $X_2$

In the subsection, the equilibrium point  $X_2$  is considered. The Jacobian matrix of system (1) at  $X_2$  is evaluated as

$$A_2 = \begin{bmatrix} -a & a & 1 & 0 \\ b - \frac{(1-\sqrt{\Delta})^2}{4a^2c} & -1 & \frac{\sqrt{\Delta}-1}{2a} & 0 \\ \frac{1-\sqrt{\Delta}}{a} & 0 & -c & 0 \\ 0 & \frac{2a^2cd(1-\sqrt{\Delta})-d(1-\sqrt{\Delta})^2}{2a^3c} & 0 & -1 \end{bmatrix} \quad (17)$$

By calculation, it is obtained that the characteristic equation of the Jacobian matrix  $A_2$  as follows

$$\tilde{\lambda}^4 + \tilde{R}_1 \tilde{\lambda}^3 + \tilde{R}_2 \tilde{\lambda}^2 + \tilde{R}_3 \tilde{\lambda} + \tilde{R}_4 = 0, \quad (18)$$

where

$$\begin{aligned} \tilde{R}_1 &= a + c + 2, \quad \tilde{R}_2 = -ab + ac + \frac{(1-\sqrt{\Delta})^2}{4ac} + 2a + 2c - \frac{1-\sqrt{\Delta}}{a} + 1, \\ \tilde{R}_3 &= -abc + \frac{(1-\sqrt{\Delta})^2}{4a} + 1 - \sqrt{\Delta} - ab + 2ac + \frac{(1-\sqrt{\Delta})^2}{4ac} + a + c - \frac{2-2\sqrt{\Delta}}{a}, \\ \tilde{R}_4 &= -abc + \frac{(1-\sqrt{\Delta})^2}{4a} + 1 - \sqrt{\Delta} + ac - \frac{1-\sqrt{\Delta}}{a}. \end{aligned} \quad (19)$$

Due to complexity and length of the eigenvalues of the Jacobian matrix  $A_2$ , the Routh-Hurwitz criterion is adopted.

According to the Routh-Hurwitz criterion, if the following conditions are satisfied:

$$\tilde{R}_1 > 0, \quad \tilde{R}_1 \tilde{R}_2 - \tilde{R}_3 > 0, \quad \tilde{R}_1 \tilde{R}_2 \tilde{R}_3 - \tilde{R}_3^2 - \tilde{R}_1^2 \tilde{R}_4 > 0, \quad \tilde{R}_4 > 0 \quad (20)$$

then all the eigenvalues of matrix  $A_2$  have negative real parts, so the equilibrium point  $X_2$  is of asymptotic stability.

### 3.4. Equilibrium Point $X_3$

Finally, the equilibrium point  $X_3$  is considered. The Jacobian matrix of system (1) at  $X_3$  is evaluated as

$$A_3 = \begin{bmatrix} -a & a & 1 & 0 \\ b - \frac{(1+\sqrt{\Delta})^2}{4a^2c} & -1 & \frac{-1-\sqrt{\Delta}}{2a} & 0 \\ \frac{1+\sqrt{\Delta}}{a} & 0 & -c & 0 \\ 0 & \frac{2a^2cd(1+\sqrt{\Delta})-d(1+\sqrt{\Delta})^2}{2a^3c} & 0 & -1 \end{bmatrix} \quad (21)$$

By calculation, it is obtained that the characteristic equation of the Jacobian matrix  $A_3$  as follows

$$\bar{\lambda}^4 + \bar{R}_1\bar{\lambda}^3 + \bar{R}_2\bar{\lambda}^2 + \bar{R}_3\bar{\lambda} + \bar{R}_4 = 0, \quad (22)$$

where

$$\begin{aligned} \bar{R}_1 &= a + c + 2, \quad \bar{R}_2 = -ab + ac + \frac{(1+\sqrt{\Delta})^2}{4ac} + 2a + 2c - \frac{1+\sqrt{\Delta}}{a} + 1, \\ \bar{R}_3 &= -abc + \frac{(1+\sqrt{\Delta})^2}{4a} + 1 + \sqrt{\Delta} - ab + 2ac + \frac{(1+\sqrt{\Delta})^2}{4ac} + a + c - \frac{2+2\sqrt{\Delta}}{a}, \\ \bar{R}_4 &= -abc + \frac{(1+\sqrt{\Delta})^2}{4a} + 1 + \sqrt{\Delta} + ac - \frac{1+\sqrt{\Delta}}{a}. \end{aligned} \quad (23)$$

Due to complexity and length of the eigenvalues of the Jacobian matrix  $A_3$ , the Routh-Hurwitz criterion is adopted.

According to the Routh-Hurwitz criterion, if the following conditions are satisfied:

$$\bar{R}_1 > 0, \quad \bar{R}_1\bar{R}_2 - \bar{R}_3 > 0, \quad \bar{R}_1\bar{R}_2\bar{R}_3 - \bar{R}_3^2 - \bar{R}_1^2\bar{R}_4 > 0, \quad \bar{R}_4 > 0 \quad (24)$$

then all the eigenvalues of matrix  $A_3$  have negative real parts, so the equilibrium point  $X_3$  is of asymptotic stability.

#### 4. Hopf Bifurcation Analysis

In this section, Hopf bifurcation of the equilibrium point  $X_0$  of system (1) is studied. At the other equilibrium points, the situations are so similar to  $X_0$  that they are not studied below.

According to the Hopf bifurcation theory, Hopf bifurcation may occur while the characteristic equation has a pair of purely imaginary eigenvalues and two eigenvalues with negative real parts. As a result, Hopf bifurcation of system (1) may occur when condition (10) satisfies

$$\lambda_1 = -1, \quad \lambda_2 = -c < 0, \quad \lambda_{3,4} = \pm\sqrt{b-1}i, \quad (25)$$

that is

$$a = -1, \quad c > 0, \quad b > 1. \quad (26)$$

Choosing the system parameters  $a = -1$ ,  $b = 2$ ,  $c = 2$ ,  $d = 1$ , then the eigenvalues  $\lambda_1 = -1$ ,  $\lambda_2 = -2$ ,  $\lambda_{3,4} = \pm i$ , where  $i = \sqrt{-1}$ . Next, Hopf bifurcation

at the point  $X_0$  is investigated with Poincaré-Birkhoff normal form theorem. The three-dimensional truncation of Equation (1) is presented as

$$\begin{aligned}\dot{X} &= \mathcal{A}X + \mathcal{F}(X), \quad X = (x, y, z, w)^T, \\ \mathcal{F}(X) &= \frac{1}{2}\mathcal{B}(X, X) + \frac{1}{6}\mathcal{C}(X, X, X) + \mathcal{O}(\|X\|^4),\end{aligned}\quad (27)$$

where

$$\mathcal{A} = \begin{bmatrix} 1 & -1 & 1 & 0 \\ 2 & -1 & 0 & 0 \\ 0 & 0 & -2 & 0 \\ 0 & 0 & 0 & -1 \end{bmatrix}, \quad \mathcal{B}(X, X) = \begin{bmatrix} 0 \\ -2xz \\ 2x^2 \\ 2y^2 \end{bmatrix}, \quad \mathcal{C}(X, X, X) = \begin{bmatrix} 0 \\ 0 \\ 0 \\ 0 \end{bmatrix}. \quad (28)$$

Letting  $Q = (q_1, q_2, q_3, q_4)^T \in \mathbb{C}^4$  be the complex eigenvector corresponding to the eigenvalue  $\lambda_3 = i$ , there exists  $P = (p_1, p_2, p_3, p_4)^T \in \mathbb{C}^4$  so that

$$\begin{aligned}\langle P, Q \rangle &= 1, & \langle P, Q \rangle &= \sum_{i=1}^4 \bar{p}_i q_i, \\ \mathcal{A}Q &= iQ, & \mathcal{A}\bar{Q} &= -i\bar{Q}, \\ \mathcal{A}^T P &= -i\omega P, & \mathcal{A}^T \bar{P} &= i\omega \bar{P}, \quad \omega \in \mathbb{C}.\end{aligned}\quad (29)$$

where and below  $\bar{\cdot}$  is represented to the conjugate symbol. According to conditions (29),  $Q$  and  $P$  are calculated as follows

$$Q = \left( \frac{1}{2} + \frac{1}{2}i, 1, 0, 0 \right)^T, \quad \bar{Q} = \left( \frac{1}{2} - \frac{1}{2}i, 1, 0, 0 \right)^T, \quad (30)$$

$$P = \left( i, \frac{1}{2} - \frac{1}{2}i, -\frac{1}{5} + \frac{2}{5}i, 0 \right)^T, \quad \bar{P} = \left( -i, \frac{1}{2} + \frac{1}{2}i, -\frac{1}{5} - \frac{2}{5}i, 0 \right)^T, \quad (31)$$

With the center manifold theorem [23] [24] [25],  $\mathbb{R}^4 = \mathbb{T}^c \oplus \mathbb{T}^{su}$ , where  $\mathbb{T}^c$  is the tangent space of  $\mathcal{P}$ ,  $\mathbb{T}^{su}$  is the residual subspace. For any  $X \in \mathbb{R}^4$ ,  $X = Y + uQ + \bar{u}\bar{Q}$ ,  $u \in \mathbb{C}$ , where  $Y \in \mathbb{T}^c$ ,  $uQ + \bar{u}\bar{Q} \in \mathbb{T}^{su}$ .  $u$  means the coordinate of  $\{\text{Re}Q, \text{Im}Q\}$  on  $\mathbb{T}^{su}$ . Due to  $\langle P, Y \rangle = 0$  and  $\langle P, \bar{Q} \rangle = 0$ , so one can get

$$\begin{aligned}u &= \langle P, X \rangle, \\ Y &= X - \langle P, X \rangle Q - \langle P, X \rangle \bar{Q}.\end{aligned}\quad (32)$$

Combining with condition (27), the coordinate variable  $u$  is developed into

$$\dot{u} = iu + \frac{1}{2}G_{20}u^2 + G_{11}u\bar{u} + \frac{1}{2}G_{02}\bar{u}^2 + u \langle P, \mathcal{B}(Q, Y) \rangle + \bar{u} \langle P, \mathcal{B}(\bar{Q}, Y) \rangle + \dots, \quad (33)$$

and the system is developed into

$$\dot{Y} = \mathcal{A}Y + \frac{1}{2}H_{20}u^2 + H_{11}u\bar{u} + \frac{1}{2}H_{02}\bar{u}^2 + \dots \quad (34)$$

where

$$\begin{aligned}G_{20} &= \langle P, \mathcal{B}(Q, Q) \rangle, \\ G_{11} &= \langle P, \mathcal{B}(Q, \bar{Q}) \rangle, \\ G_{02} &= \langle P, \mathcal{B}(\bar{Q}, \bar{Q}) \rangle,\end{aligned}$$

$$\begin{aligned}
 H_{20} &= \mathcal{B}(Q, Q) - \langle P, \mathcal{B}(Q, Q) \rangle Q - \langle \bar{P}, \mathcal{B}(Q, Q) \rangle \bar{Q}, \\
 H_{11} &= \mathcal{B}(Q, \bar{Q}) - \langle P, \mathcal{B}(Q, \bar{Q}) \rangle Q - \langle \bar{P}, \mathcal{B}(Q, \bar{Q}) \rangle \bar{Q}, \\
 H_{02} &= \mathcal{B}(\bar{Q}, \bar{Q}) - \langle P, \mathcal{B}(\bar{Q}, \bar{Q}) \rangle Q - \langle \bar{P}, \mathcal{B}(\bar{Q}, \bar{Q}) \rangle \bar{Q},
 \end{aligned} \tag{35}$$

$$\mathcal{B}(X, Y) = \begin{bmatrix} 0 \\ -xz' - zx' \\ 2xx' \\ 2yy' \end{bmatrix}, \quad X = \begin{bmatrix} x \\ y \\ z \\ w \end{bmatrix}, \quad Y = \begin{bmatrix} x' \\ y' \\ z' \\ w' \end{bmatrix}. \tag{36}$$

Since  $\bar{H}_{20} = H_{02}$ ,  $\bar{H}_{11} = H_{11}$ , without losing generality, the main order of  $Y$  can be expressed as

$$\begin{aligned}
 Y &= \mathcal{W}(u, \bar{u}) + \mathcal{O}(\|u\|^3), \\
 \mathcal{W}(u, \bar{u}) &\equiv \frac{1}{2}W_{20}u^2 + W_{11}u\bar{u} + \frac{1}{2}W_{02}\bar{u}^2,
 \end{aligned} \tag{37}$$

and

$$\langle P, W_{20} \rangle = 0, \quad \langle P, W_{11} \rangle = 0, \quad \langle P, W_{02} \rangle = 0. \tag{38}$$

Considering condition (34) and  $\dot{Y} = \frac{\partial \mathcal{W}(u, \bar{u})}{\partial u} \dot{u} + \frac{\partial \mathcal{W}(u, \bar{u})}{\partial \bar{u}} \dot{\bar{u}}$ , it can be obtained that constraint conditions is as the following

$$\begin{cases} W_{20} = (2iI - \mathcal{A})^{-1} H_{20}, \\ W_{11} = -\mathcal{A}^{-1} H_{11}, \\ W_{02} = (-2iI - \mathcal{A})^{-1} H_{02}. \end{cases} \tag{39}$$

On those conditions the restricted condition of coordinate variable is shown as

$$\begin{aligned}
 \dot{u} &= iu + \frac{1}{2}G_{20}u^2 + G_{11}u\bar{u} + \frac{1}{2}G_{02}\bar{u}^2 \\
 &+ \frac{1}{2} \left( 2\langle P, \mathcal{B}(Q, W_{11}) \rangle + \langle P, \mathcal{B}(\bar{Q}, W_{20}) \rangle \right) z^2 \bar{z} + \dots.
 \end{aligned} \tag{40}$$

Next, by substituting conditions (30), (31) into conditions (35), (36), (39), the specific results of those expressions are given as follows

$$\mathcal{B}(Q, Q) = \begin{bmatrix} 0 \\ 0 \\ i \\ 2 \end{bmatrix}, \quad \mathcal{B}(Q, \bar{Q}) = \begin{bmatrix} 0 \\ 0 \\ 1 \\ 2 \end{bmatrix}, \quad \mathcal{B}(\bar{Q}, \bar{Q}) = \begin{bmatrix} 0 \\ 0 \\ -i \\ 2 \end{bmatrix}, \tag{41}$$

$$G_{20} = \frac{2}{5} - \frac{1}{5}i, \quad G_{11} = -\frac{1}{5} - \frac{2}{5}i, \quad G_{02} = -\frac{2}{5} + \frac{1}{5}i, \tag{42}$$

$$H_{20} = \left( -\frac{1}{5}i, \frac{2}{5}i, i, 2 \right)^T, \tag{43}$$

$$H_{11} = \left( -\frac{1}{5}, \frac{2}{5}, 1, 2 \right)^T, \tag{44}$$

$$H_{02} = \left( \frac{1}{5}i, -\frac{2}{5}i, -i, 2 \right)^T, \quad (45)$$

$$W_{20} = \left( -\frac{1}{20} - \frac{1}{20}i, \frac{1}{10} + \frac{1}{10}i, \frac{1}{4} + \frac{1}{4}i, \frac{2}{5} - \frac{4}{5}i \right)^T, \quad (46)$$

$$W_{11} = \left( -\frac{1}{10}, \frac{1}{5}, \frac{1}{2}, 2 \right)^T, \quad (47)$$

$$W_{02} = \left( -\frac{1}{20} + \frac{1}{20}i, \frac{1}{10} - \frac{1}{10}i, \frac{1}{4} - \frac{1}{4}i, \frac{2}{5} + \frac{4}{5}i \right)^T, \quad (48)$$

Therefore the first Lyapunov coefficient is

$$\begin{aligned} L_1(0) &= -\operatorname{Re} \left\langle P, \mathcal{B} \left( Q, \mathcal{A}^{-1} \mathcal{B} \left( Q, \bar{Q} \right) \right) \right\rangle \\ &\quad + \frac{1}{2} \operatorname{Re} \left\langle P, \mathcal{B} \left( \bar{Q}, (2iI - \mathcal{A})^{-1} \mathcal{B} \left( Q, Q \right) \right) \right\rangle \\ &= -\frac{1}{80} < 0, \end{aligned} \quad (49)$$

in which we can see the Hopf bifurcation is supercritical at the point  $X_0(0, 0, 0, 0)$ .

## 5. Numerical Simulations

In the section, the time histories, Lyapunov exponential spectrums, projections of four-dimensional phase portrait and bifurcation diagrams are studied by numerical simulation. By considering the same initial value  $(0.01, 0, 0, 0)$  and different situations which depend on different parameters  $a$ ,  $b$ ,  $c$ , and  $d$ , using the fourth-order Runge-Kutta method, numerical simulations including time histories, Lyapunov exponential spectrums and projections of phase portrait verify the results of the above analysis. And the ways to enter chaos can be seen through bifurcation diagrams.

Choosing parameters  $a = -0.9$ ,  $b = 2$ ,  $c = 2$  and  $d = 1$ , the time histories, Lyapunov exponential spectrums, two-dimensional projections and three-dimensional projections of four-dimensional phase portrait are shown in **Figures 1-4**. From **Figure 1** and **Figure 2** one can see the system in this situation is in an asymptotically stable state. From **Figure 3** and **Figure 4** one can know the system motion gradually converges to the equilibrium point  $X_0(0, 0, 0, 0)$  as time goes by, which verifies the analytical results.

Choosing parameters  $a = -1$ ,  $b = 2$ ,  $c = 2$  and  $d = 1$ , the time histories, Lyapunov exponential spectrums, two-dimensional projections and three-dimensional projections of four-dimensional phase portrait are shown in **Figures 5-8**. From **Figures 5-8**, one can see the system in this situation is under periodic motions and is also in a stable state. In the situation, there will occur the Hopf bifurcations in the system if the system is subjected to minor disturbance, which verifies the theoretical analysis in Section 4.

Choosing parameters  $a = 12$ ,  $b = 45$ ,  $c = 4$  and  $d = 1$ , the time histories, Lyapunov exponential spectrums, two-dimensional projections and three-dimensional projections of four-dimensional phase portrait are shown in **Figures**

9-12. From **Figure 9** one can see time histories are in a disordered state. **Figure 10** shows that the system in this situation is hyperchaotic. From **Figure 11** one can see plane projection on  $x-y$  plane is a family of quasi symmetric cumulative bicyclo and plane projection on  $z-w$  plane is in disorder. From **Figure 11** one can see spatial projection in  $x-y-z$  space and spatial projection in  $x-y-w$  space are in a chaotic state.

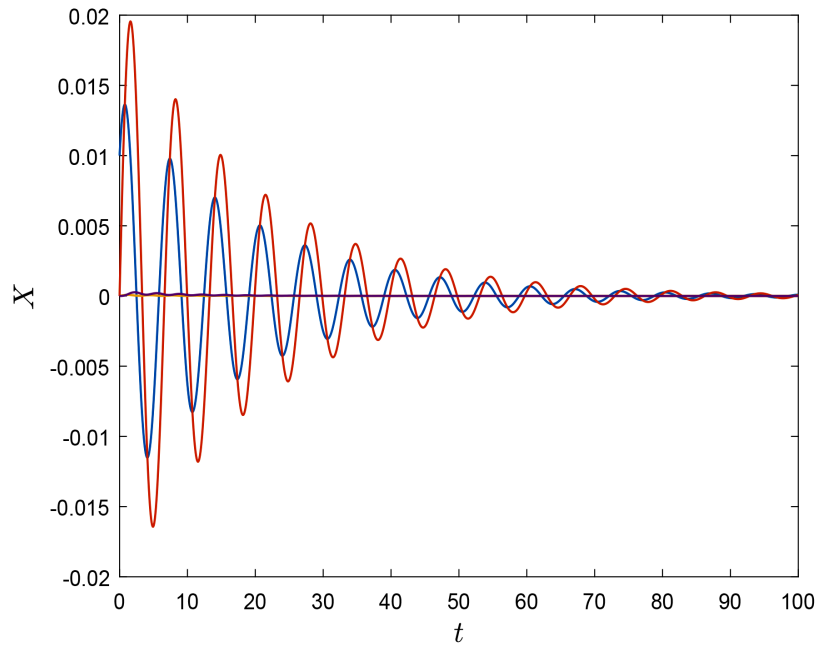


**Figure 1.** The time histories for  $(a,b,c,d) = (-0.9,2,2,1)$ .

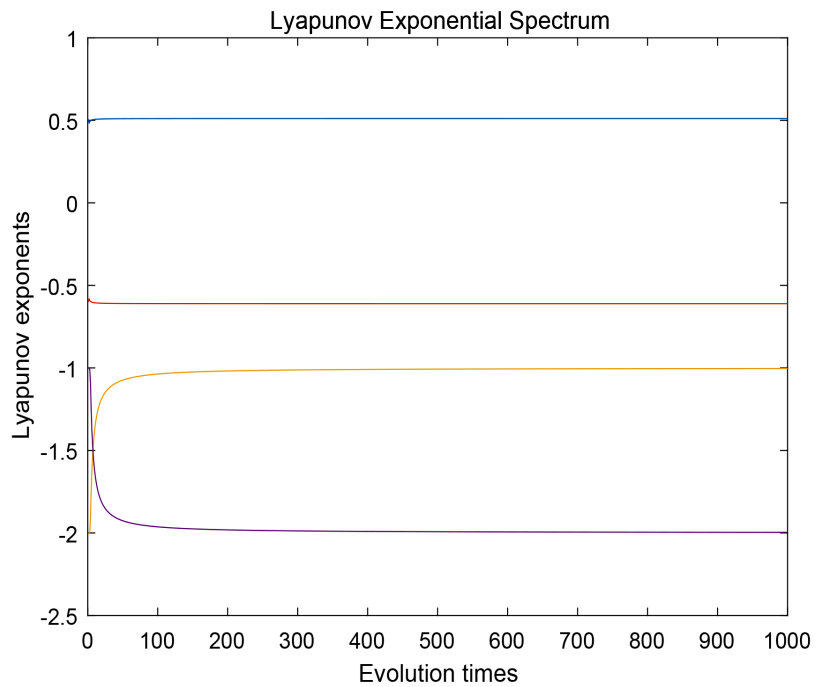


**Figure 2.** The Lyapunov exponential spectrum for  $(a,b,c,d) = (-0.9,2,2,1)$ .

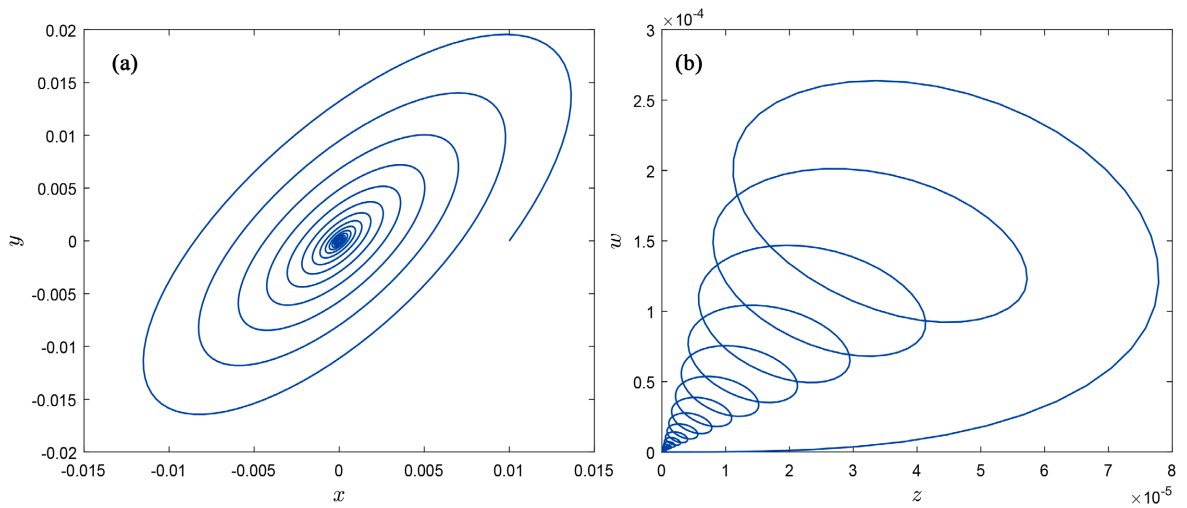


**Figure 3.** two-dimensional projections of four-dimensional phase portrait for  $(a,b,c,d) = (-0.9, 2, 2, 1)$ . (a) Plane projection projected on  $x-y$  plane; (b) plane projection projected on  $z-w$  plane.

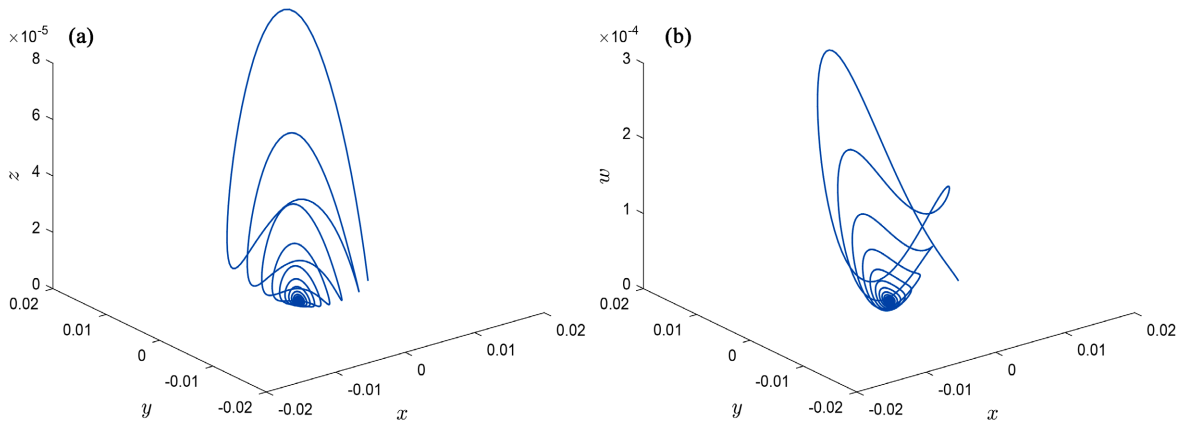


**Figure 4.** Three-dimensional projections of four-dimensional phase portrait for  $(a,b,c,d) = (-0.9, 2, 2, 1)$ , (a) spatial projection projected in  $x-y-z$  space; (b) spatial projection projected in  $x-y-w$  space.

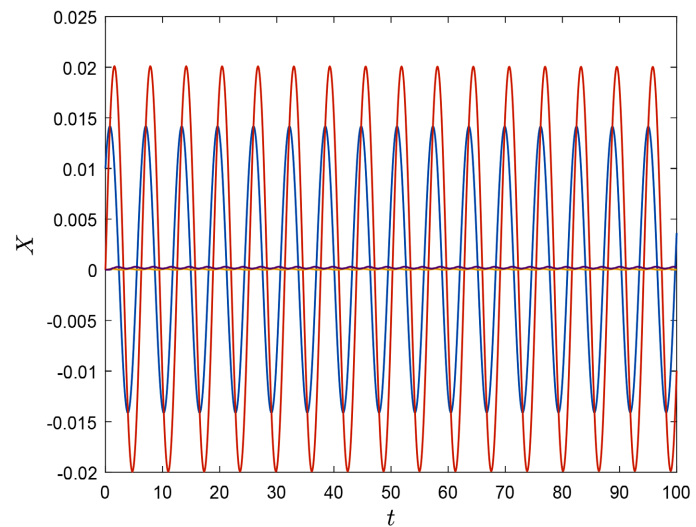


**Figure 5.** The time histories for  $(a,b,c,d) = (-1, 2, 2, 1)$ .

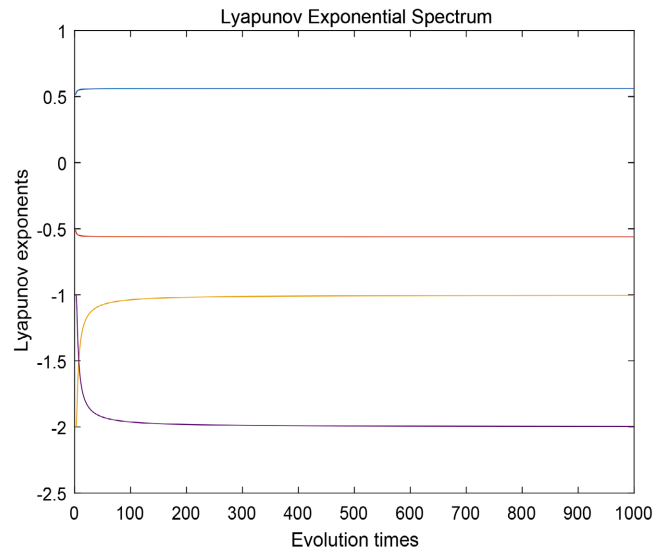


**Figure 6.** The Lyapunov exponential spectrum for  $(a,b,c,d) = (-1, 2, 2, 1)$ .

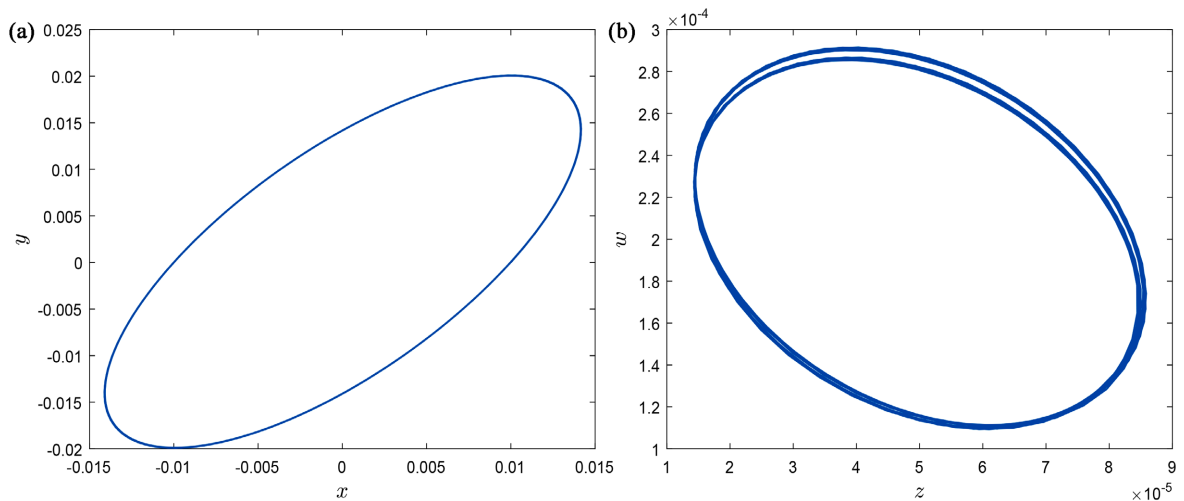


**Figure 7.** Two-dimensional projections of four-dimensional phase portrait for  $(a,b,c,d) = (-1, 2, 2, 1)$ . (a) Plane projection projected on  $x$ - $y$  plane; (b) plane projection projected on  $z$ - $w$  plane.

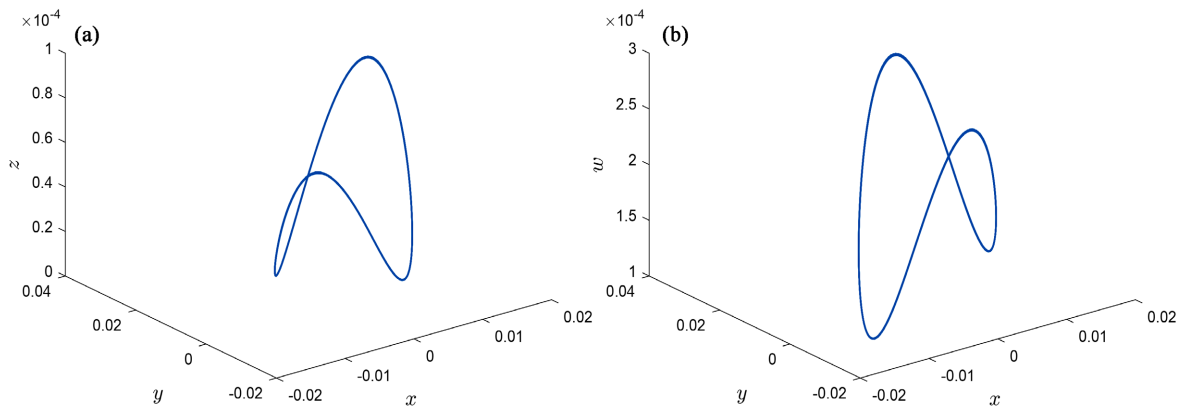


**Figure 8.** Three-dimensional projections of four-dimensional phase portrait for  $(a,b,c,d) = (-1, 2, 2, 1)$ . (a) Spatial projection projected in  $x$ - $y$ - $z$  space; (b) spatial projection projected in  $x$ - $y$ - $w$  space.

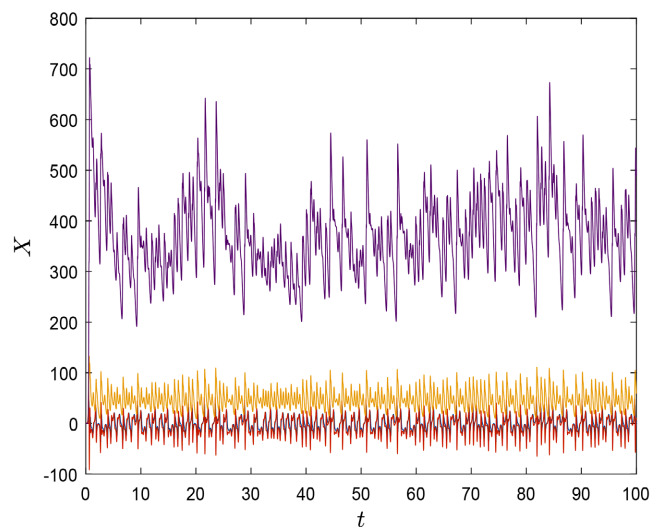


**Figure 9.** The time histories for  $(a, b, c, d) = (15, 25, 5, 1)$ .

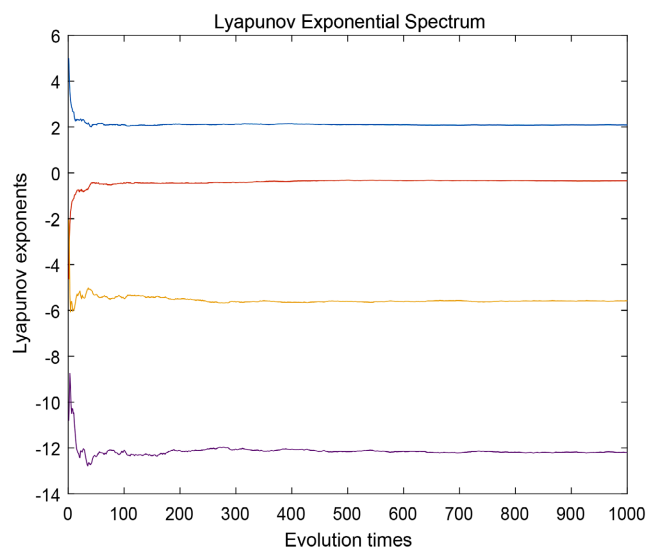


**Figure 10.** The Lyapunov exponential spectrum for  $(a, b, c, d) = (15, 25, 5, 1)$ .

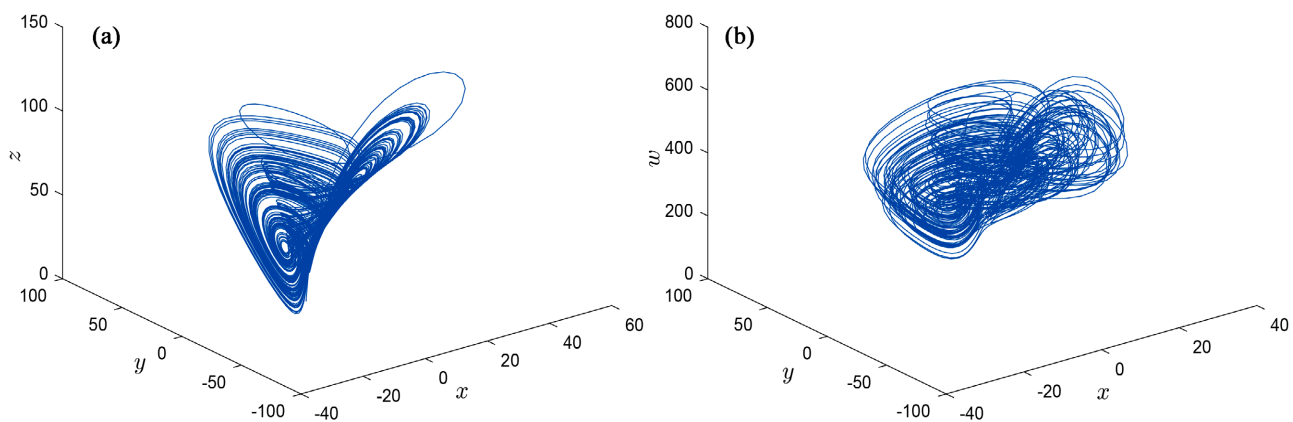


**Figure 11.** Two-dimensional projections of four-dimensional phase portrait for  $(a, b, c, d) = (15, 25, 5, 1)$ . (a) Plane projection projected on  $x$ - $y$  plane; (b) plane projection projected on  $z$ - $w$  plane.

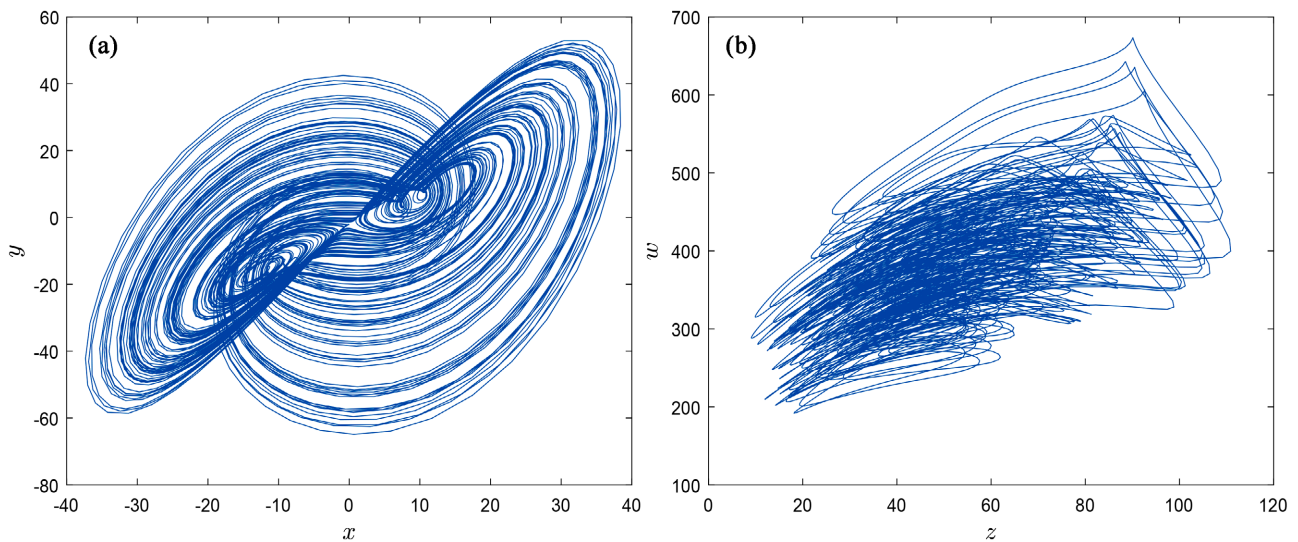


**Figure 12.** Three-dimensional projections of four-dimensional phase portrait for  $(a, b, c, d) = (15, 25, 5, 1)$ . (a) Spatial projection projected in  $x$ - $y$ - $z$  space; (b) spatial projection projected in  $x$ - $y$ - $w$  space.

## 6. Conclusion

With analytical and numerical methods, stability and Hopf bifurcation analysis of a new four-dimensional autonomous system are investigated in this manuscript. Determining conditions of equilibrium points on different parameters are derived at the beginning. Next stability conditions and bifurcation conditions are investigated successively. It is found that Hopf bifurcation on the initial point is supercritical in this four-dimensional autonomous system. The theoretical results are verified by numerical simulation. Besides, the new four-dimensional autonomous system under the parametric conditions of hyperchaos is investigated in detail. It is found that the system can enter hyperchaos, first through Hopf bifurcation and then through periodic bifurcation.

## Acknowledgments

The project was supported by National Natural Science Foundation of China (11772148, 11872201, 12172166) and China Postdoctoral Science Foundation (2013T60531).

## Conflicts of Interest

The authors declare no conflicts of interest regarding the publication of this paper.

## References

- [1] Hagrass, E.A.A. and Saber, M. (2020) Low Power and High-Speed FPGA Implementation for 4D Memristor Chaotic System for Image Encryption. *Multimedia Tools and Applications*, **79**, 23203-23222. <https://doi.org/10.1007/s11042-019-08517-w>
- [2] Zhu, H., Ge, J., Qi, W., Zhang, X. and Lu, X. (2022) Dynamic Analysis and Image Encryption Application of a Sinusoidal-Polynomial Composite Chaotic System. *Ma-*

- thematics and Computers in Simulation*, **198**, 188-210.  
<https://doi.org/10.1016/j.matcom.2022.02.029>
- [3] Li, H., Wang, L. and Lai, Q. (2021) Synchronization of a Memristor Chaotic System and Image Encryption. *International Journal of Bifurcation and Chaos*, **31**, Article ID: 2150251. <https://doi.org/10.1142/S0218127421502515>
- [4] Xian, Y., Wang, X., Teng, L., Yan, X., Li, Q. and Wang, X. (2022) Cryptographic System Based on Double Parameters Fractal Sorting Vector and New Spatiotemporal Chaotic System. *Information Sciences*, **596**, 304-320.  
<https://doi.org/10.1016/j.ins.2022.03.025>
- [5] Guo, H., Zhang, X., Zhao, X., Yu, H. and Zhang, L. (2020) Quadratic Function Chaotic System and Its Application on Digital Image Encryption. *IEEE Access*, **8**, 55540-55549. <https://doi.org/10.1109/ACCESS.2020.2981771>
- [6] Fan, H., Lu, H., Zhang, C., Li, M. and Liu, Y. (2022) Cryptanalysis of an Image Encryption Algorithm Based on Random Walk and Hyperchaotic Systems. *Entropy*, **24**, 40. <https://doi.org/10.3390/e24010040>
- [7] Li, X., Mou, J., Cao, Y. and Banerjee, S. (2022) An Optical Image Encryption Algorithm Based on a Fractional-Order Laser Hyperchaotic System. *International Journal of Bifurcation and Chaos*, **32**, Article ID: 2250035.  
<https://doi.org/10.1142/S0218127422500353>
- [8] Samiullah, M., *et al.* (2020) An Image Encryption Scheme Based on DNA Computing and Multiple Chaotic Systems. *IEEE Access*, **8**, 25650-25663.  
<https://doi.org/10.1109/ACCESS.2020.2970981>
- [9] Liu, L., Wang, D. and Lei, Y. (2020) An Image Encryption Scheme Based on Hyper Chaotic System and DNA With Fixed Secret Keys. *IEEE Access*, **8**, 46400-46416.  
<https://doi.org/10.1109/ACCESS.2020.2978492>
- [10] Gao, X., Yu, J., Banerjee, S., Yan, H. and Mou, J. (2021) A New Image Encryption Scheme Based on Fractional-Order Hyperchaotic System and Multiple Image Fusion. *Scientific Reports*, **11**, Article No. 15737.  
<https://doi.org/10.1038/s41598-021-94748-7>
- [11] Lv, Y. (2022) The Spatially Homogeneous Hopf Bifurcation Induced Jointly by Memory and General Delays in a Diffusive System. *Chaos, Solitons & Fractals*, **156**, Article ID: 111826. <https://doi.org/10.1016/j.chaos.2022.111826>
- [12] Efran, I.J. and Manuel, J.L. (2022) Robust Tracking-Surveillance and Landing over a Mobile Target by Quasi-Integral-Sliding Mode and Hopf Bifurcation. *Journal of the Franklin Institute*, **359**, 2120-2155. <https://doi.org/10.1016/j.jfranklin.2021.12.017>
- [13] Li, J., Wu, H. and Cui, N. (2020) Bifurcation, Chaos, and Their Control in a Wheelset Model. *Mathematical Methods in the Applied Sciences*, **43**, 7152-7174.  
<https://doi.org/10.1002/mma.6454>
- [14] Wang, W., Liu, Z. and Yang, R. (2022) Hopf Bifurcation Analysis of a Delayed Diffusive Predator-Prey Model with Predator Interference or Foraging Facilitation. *Discrete Dynamics in Nature and Society*, **2022**, Article ID: 5278036.  
<https://doi.org/10.1155/2022/5278036>
- [15] Huang, Y., Zhang, H. and Niu, B. (2022) Resonant Double Hopf Bifurcation in a Diffusive Ginzburg-Landau Model with Delayed Feedback. *Nonlinear Dynamics*, **108**, 2223-2243. <https://doi.org/10.1007/s11071-022-07339-0>
- [16] Shiva, E., Reza, K.G. and Alireza, A. (2020) Hopf Bifurcation, Chaos Control and Synchronization of a Chaotic Fractional-Order System with Chaos Entanglement Function. *Mathematics and Computers in Simulation*, **172**, 321-340.  
<https://doi.org/10.1016/j.matcom.2019.11.009>

- [17] Wang, J., Shi, H., Xu, L. and Zang, L. (2022) Hopf Bifurcation and Chaos of Tumor-Lymphatic Model with Two Time Delays. *Chaos, Solitons & Fractals*, **157**, Article ID: 111922. <https://doi.org/10.1016/j.chaos.2022.111922>
- [18] Ramesh, P., Sambath, M. and Balachandran, K. (2022) Hopf Bifurcation and Synchronisation of a Fractional-Order Butterfly-Fish Chaotic System. *Journal of Control and Decision*, **9**, 117-128. <https://doi.org/10.1080/23307706.2021.1920485>
- [19] Amin, Z. and Saeed, T. (2016) Hopf Bifurcation Analysis and Ultimate Bound Estimation of a New 4-D Quadratic Autonomous Hyper-Chaotic System. *Applied Mathematics and Computation*, **291**, 323-339. <https://doi.org/10.1016/j.amc.2016.07.023>
- [20] Calderon-Saavedra, P., Munoz-Aguirre, E., Alvarez-Mena, J. and Gomez-Perez, S. (2018) Hopf Bifurcation Control in a Lorenz Type System. *Journal of Applied Mathematics and Physics*, **6**, 1704-1719. <https://doi.org/10.4236/jamp.2018.68146>
- [21] Verdugo, A. (2018) Hopf Bifurcation Analysis of the Repressilator Model. *American Journal of Computational Mathematics*, **8**, 137-152. <https://doi.org/10.4236/ajcm.2018.82011>
- [22] Fang, P., Huang, L., Lou, M., Jiang, K. and Wu, C. (2022) Color Image Encryption Algorithm Based on Four-Dimensional Superchaotic Systems. *Computer Engineering and Design*, **43**, 361-369. (In Chinese)
- [23] Zhou, L.L., Chen, Z., Wang, Z. and Wang, J. (2016) On the Analysis of Local Bifurcation and Topological Horseshoe of a New 4D Hyper-Chaotic System. *Chaos, Solitons & Fractals*, **91**, 148-156. <https://doi.org/10.1016/j.chaos.2016.05.017>
- [24] Zhou, L., Zhao, Z. and Chen, F. (2020) Stability and Hopf Bifurcation Analysis of a New Four-Dimensional Hyper-Chaotic System. *Modern Physics Letters B*, **34**, Article ID: 2050327. <https://doi.org/10.1142/S0217984920503273>
- [25] Zhou, L. and Kabbah, A. (2022) Hopf Bifurcation and Its Control in a 3D Autonomous System. *The European Physical Journal Special Topics*, **231**, 2115-2124. <https://doi.org/10.1140/epjs/s11734-022-00488-8>